Full length article

MHC II-β chain gene expression studies define the regional organization of the thymus in the developing bony fish *Dicentrarchus labrax* (L.)

S. Picchietti[a]

L. Abelli[b,*]

abl@unife.it

L. Guerra[a]

E. Randelli[a]

F. Proietti Serafini[a]

M.C. Belardinelli[a]

F. Buonocore[a]

C. Bernini[a]

A.M. Fausto[a]

G. Scapigliati[a]

[a]Dep. for Innovation in Biological, Agro-food and Forest Systems, Tuscia University, Viterbo, Italy

[b]Dep. Life Sciences & Biotechnology, University of Ferrara, Via Borsari 46, Ferrara 441241, Italy

*Corresponding author. Fax: +39 0761 455715.

Abstract

MHC II-β chain gene transcripts were quantified by real-time PCR and localised by *in situ* hybridization in the developing thymus of the teleost *Dicentrarchus labrax*, regarding the specialization of the thymic compartments.

MHC II-β expression significantly rose when the first lymphoid colonization of the thymus occurred, thereafter increased further when the organ progressively developed cortex and medulla regions. The evolving patterns of *MHC II-β* expression provided anatomical insights into some mechanisms of thymocyte selection. Among the stromal cells transcribing *MHC II-β*, scattered cortical epithelial cells appeared likely involved in the positive selection, while those abundant in the cortico-medullary border and medulla in the negative selection. These latter most represent dendritic cells, based on typical localization and phenotype.

These findings provide further proofs that efficient mechanisms leading to maturation of naïve T cells are operative in teleosts, strongly reminiscent of the models conserved in more evolved gnathostomes.

Keywords: MHC II; Dendritic cells; Thymic epithelial cells; Thymus; Teleost

Abbreviations: APCs, antigen presenting cells; BSA, bovine serum albumin; CK, cytokeratin; CMB, cortico-medullary border; Ct, threshold cycle; cTECs, cortical thymic epithelial cells; DCs, dendritic cells; DEPC, diethylpyrocarbonate; dph, days post-hatching; EDTA, ethylenediaminetetraacetic acid; IHC, immunohistochemistry; IR, immunoreactive; ISH, *in situ* hybridization; mAb, monoclonal antibody; mTECs, medullary thymic epithelial cells; PBS, phosphate-buffered saline; PCNA, proliferating cell nuclear antigen; RT-PCR, reverse transcriptase-polymerase chain reaction; SDS, sodium dodecylsulfate; SSC, saline-sodium citrate; TECs, thymic epithelial cells

1 Introduction

The thymus represents a crucial component of the adaptive immune system being the primary lymphoid organ for the maturation and release of naïve T cells ~~(Arnason et al. 1961,~~ [3,4,38]). In all gnathostome vertebrates the thymus originates as epithelial buds, with the participation of different embryonic layers and neural crest cells, in the pharyngeal pouches later colonised by lymphoid progenitors coming from primordial haematopoietic organs [5]. In teleost bony fish, is a

paired organ located dorsally, often protruding into the gill chambers, separated by the water only by a mucosal epithelium [34,63]. The thymus has highly variable structure among species [7] but always contains distinct stromal cells and lymphoid cells (thymocytes) undergoing maturation. The stromal cells are distributed in an ordered fashion that defines the histological architecture of the thymus and provides the appropriate microenvironments for thymocyte differentiation [33]. Similarly to more evolved vertebrates, different compartments of the teleost thymus are apparently specialised to support various differentiation steps, however a complete understanding of the processes that control the cellular interactions among thymoctes and stromal populations to accomplish major steps, such as lineage commitment and selection, remains an important issue for future research.

Evidence about the occurrence of different compartments in the teleost thymus, with specific roles in differentiation pathways, has derived from studies in juveniles of the European sea bass *Dicentrarchus labrax* (L.) [1,41,42] that provided insights into mechanisms of thymocyte selection. Also in the Atlantic halibut developing T cells rely on a functional zonation of the thymus in cortical, cortico-medullary, and medullary regions that constitute throughout organogenesis [40]. Other studies in trout [55] and clonal ginbuna crucian carp [56,57] have confirmed the existence in teleosts of $CD4^+$ and $CD8\text{-}\alpha^+$ T cell subsets, whose morphology, tissue distribution and gene expression patterns were similar to mammalian counterparts, although their differentiation processes await further investigation.

The stepwise progression of mammalian thymocyte maturation requires serial migration through distinct thymic regions, where interactions with cortical and medullary subsets of thymic epithelial cells (TECs) and other stromal populations take place. Stromal TECs play a major role in thymocyte positive selection by presenting self-peptides on self-MHC molecules. The *MHC* genes encode for class I and class II membrane-bound glycoproteins, responsible for binding antigenic determinants. Studies in mammals have clearly demonstrated that CD^{4+} thymocytes undergo maturation through cell–cell interaction with TECs expressing MHC class II molecules [37]. In teleosts, *MHC class I* and *class II* loci reside in different linkage groups ~~(Stet et al., 2003)~~ [52] and *MHC II* genes have been identified in many species [12,16,19,22,35,39,44,47,49,51–53,61] including the European sea bass [9]. As in cartilaginous fish, teleost MHC II is a heterodimer with α and β chains, expressed on the surface of only a few cell types. MHC class II expression was first demonstrated in a teleost species (Atlantic salmon) with specific antibodies that immunostained epithelial cells and cells scattered in haematopoietic tissues (lymphocytes, macrophages and dendritic-like cells) [31]. Later studies revealed high *MHC class II* transcripts in acidophilic granulocytes of *Sparus aurata* [14] and surface MHC class II molecules in dendritic cells (DCs) of rainbow trout [6], suggesting that these cell types could represent in teleosts specialized antigen presenting cells (APCs).

This paper first describes in sea bass the localization of *MHC class II* transcripts in the developing thymus and regards the events that lead to the formation of thymic microenvironments. We report about the occurrence in the teleost thymus of *MHC II* expressing stromal cells strongly reminiscent of TECs and DCs characterised in more evolved vertebrates, and likely involved in thymocyte differentiation and selection.

2 Materials and methods

2.1 Fish

Sea bass reared at 15 ± 1 °C were provided by the Aquaculture station "Nuova Azzurro", Civitavecchia (Italy). The embryos hatched at day 2 after fertilization and were fed with *Artemia salina* nauplii for 3–4 weeks from 8 days post hatching (dph), followed by Proton pellets (INVE, Belgium). Released eggs, larvae (from 2 to 32 dph), post-larvae (from 39 to 92 dph) and 1 year-old juveniles (still sexually immature) were sampled. Fish were anaesthetised with 0.03% tricaine methane sulphonate in water before sampling.

2.2 Polymerase chain reaction

Total RNA was extracted from released eggs and three pools per stage (N = 5 specimens each) sampled at 2, 4, 6, 8, 13, 16, 21, 25, 32, 39, 51, 62, 75 and 92 dph, and from the thymus of 1 year-old specimens. Specimens from 16 dph on were dissected to eliminate the cranial region with the eyes and the postanal region of the body. After grinding the tissues with a sterile pestle in 2-ml tubes, one ml of Tripure (Roche, Germany) was added in each tube to the cells. RNA was suspended in diethylpyrocarbonate (DEPC; Sigma–Aldrich, Germany) treated water and reverse transcriptase-polymerase chain reaction (RT-PCR) was performed using Ready-To-Go RT-PCR beads following manufacturer's instructions. To check the RNA quality and quantity, RT-PCRs were performed using specific primers for sea bass *β-actin* that bracketed an intron [10] to verify the absence of DNA contamination by the size of the obtained amplicons (550 bp in case of no intron, a doublet around 1000 bp with intron, primers: ACRFW 5′-ATCGTGGGGCGCCCCAGGCACA-3′; ACTRV: 5′-CTCCTTAATGTCACGCACGATTTC-3′). The cycling protocol was: 1 cycle of 94 °C for 5 min, 35 cycles of 94 °C for 45 s, 55 °C for 45 s and 72 °C for 45 s, followed by 1 cycle of 72 °C for 10 min. *MHC II-β* gene expression was studied using specific primers (Table 1a) designed to amplify a 316 bp product of sea bass *MHC II-β chain* sequence [9]. The cycling protocol was: 1 cycle of 94 °C for 5 min, 35 cycles of 94 °C for 45 s, 55 °C for 45 s and 72 °C for 45 s, followed by 1 cycle of 72 °C for 10 min. PCR products were purified from agarose gel using the QIAquick Gel Extraction Kit (QIAgen, Milano, Italy) and directly sequenced with the MWG sequencing services to confirm identity of transcripts.

Table 1 Specific primers used for RT-PCR (~~1~~a), real-time PCR (~~1~~b) and ISH analysis (~~1~~c) primers for RT-PCR and sense and anti-sense RNA probes).

a)	
RT-PCR	**Primer sequences (5′–3′)**
Forward	**TCAGAGTGAGCTGGCTCAGA**

Reverse	GGAACCAGAATCCTTCCTGG

b)

Real-time PCR	Primer sequences (5′–3′)
Forward	CAGAGACGGACAGGAAG
Reverse	CAAGATCAGACCCAGGA

c)

ISH	Sequences (5′–3′)
RT-PCR forward	CATCCCTCCATGTTGGTCTG
RT-PCR reverse	GGATTCTGGTTCCCAGTAAC
Sense probe forward	TAATACGACTCACTATAGGG
Sense probe reverse	GGATTCTGGTTCCCAGTAAC
Anti-sense probe forward	CATCCCTCCATGTTGGTCTG
Anti-sense probe reverse	GCATTTAGGTGACACTATAGAATAG

2.3 Real-time polymerase chain reaction

Total RNA was isolated with Tripure (Roche), following the manufacturer's instructions, from three pools per stage (*N* = 5 specimens each) of larvae and post-larvae, and from the thymus of four 1 year-old juveniles. RNA was suspended in DEPC treated water and used for real-time PCR. Controls for the presence of DNA contamination were performed using sea bass *β-actin* primers that bracketed an intron. For reverse transcription, the BioScript RNase H minus enzyme (Bioline) was used as follows: 2 μg of total RNA was mixed with 1 μl of random hexamer (0.2 μg/μl; GE Healthcare Life Sciences) and nuclease free water was added to a final volume of 12 μl. This mixture was incubated at 70 °C for 5 min, then cooled on ice. Later, 0.4 μl of a reaction mix containing 100 mM dNTPs (25 mM each; Promega), 4 μl of 5× Reaction buffer, nuclease free water to a final volume of 19.75 μl and 0.25 μl of BioScript at 200 U/μl were added and the solution incubated at 25 °C for 10 min, then at 37 °C for 60 min. The reaction was stopped by heating at 70 °C for 10 min.

MHC II-β transcripts were quantified with a Mx3000P™ real-time PCR system (Stratagene) equipped with version 2.02 software and using the Brilliant SYBR Green Q-PCR Master Mix (Stratagene) following the manufacturer's instructions. ROX™ was used as internal passive reference dye since it is not reactive during real-time PCR therefore can be used to normalize slight differences in the volume of the added real-time PCR reaction, transparency of the plastic caps and other sources of differences among wells.

Specific PCR primers (Table 1b) were designed for the amplification of products (~200 bp) from the constant region of *MHC II-β* and *β-actin* as house-keeping gene. Ten nanograms of cDNA template were used in each PCR reaction. The PCR conditions were as follows: 95 °C for 10 min, followed by 35 cycles of 95 °C for 45 s, 52 °C for 45 s and 72 °C for 45 s. Reactions were performed in triplicate for each template cDNA, that was replaced with water in all blank control reactions. Each run was terminated with a melting curve analysis which resulted in a melting peak profile specific for the amplified target DNA. The analysis was carried out using the endpoints method option of the Mx3000P™ software that allows the fluorescence data at the end of each extension stage of amplification to be collected.

2.4 Quantification of cDNA

A relative quantification was performed comparing the levels of the target transcript to a reference transcript. For developmental studies, the pool (16 dph larvae) with the lowest amount of *MHC II-β* transcript was used as unitary calibrator. A normaliser target (*β-actin*) was included in the analysis to correct for differences in total cDNA input among the different samples. Quantitative assessment was based on determination of threshold cycle (Ct), defined as the cycle at which fluorescence increased significantly over background value. The size and specificity of the real-time PCR products was checked by agarose gel electrophoresis and sequencing, respectively.

2.5 In situ hybridization (ISH)

2.5.1 Synthesis of RNA probes

Cells from thymus of sea bass juveniles (20–30 g) were obtained by tissue teasing and suspended in Tripure (Roche). Total RNA was extracted following manufacturer's instructions and isolated in DEPC treated water. RT-PCR was performed with Ready-To-Go RT-PCR beads (Amersham) using 1 µg total RNA and 0.5 µg random primers [pd(N)$_6$] in a total 50 µl volume. The primers (Table 1c) were designed to amplify a 373 bp product corresponding to the constant region of sea bass *MHC II-β chain* [9]. Reactions were run using the Mastercycler personal (Eppendorf). The cycling protocol was: 1 cycle of 94 °C for 5 min, 35 cycles of 94 °C for 45 s, 55 °C for 45 s, 72 °C for 45 s, followed by 1 cycle of 72 °C for 10 min. PCR products (15 µl) were visualised on 1% agarose gels containing ethidium bromide (10 ng/ml) using Hyperladder IV (Bioline) as size marker. DNA amplified by PCR was purified using the QIAquick Gel Extraction Kit (QIAgen), inserted into the pGEM-T Easy vector (Promega) and transfected into competent JM109 *Escherichia coli* cells. Plasmid DNA from three independent clones was purified using the Wizard Plus SV Minipreps DNA Purification System (Promega) and sequenced using MWG DNA Sequencing Services. Sequences generated were analysed for similarity with other known sequences using the BLAST program.

The anti-sense probe was obtained using the selected plasmid clone as target in a PCR reaction (see primers in Table 1c). The cycling protocol was: 1 cycle of 94 °C for 5 min, 35 cycles of 94 °C for 45 s, 48 °C for 45 s, 72 °C for 45 s, followed by 1 cycle of 72 °C for 10 min. The sense probe (for negative control of ISH) was obtained using the selected plasmid clone as target in a PCR reaction (see primers in Table 1c). The cycling protocol was: 1 cycle of 94 °C for 5 min, 35 cycles of 94 °C for 45 s, 54 °C for 45 s, 72 °C for 45 s, followed by 1 cycle of 72 °C for 10 min. The fragments obtained were purified by Quick Clean Kit (Bioline) and used to synthesize digoxigenin-~~labeled~~ labelled RNA probes with the DIG-RNA Labeling Kit (Roche) following manufacturer's instructions.

2.5.2 Staining procedures

Whole larvae and post-larvae, and dissected thymus from 1 year-old specimens (*N* = 20) were fixed overnight at room temperature in 4% paraformaldehyde in 0.01 M, pH 7.4 phosphate-buffered saline (PBS) and gradually dehydrated before paraffin wax embedding. Serial sections (5 µm) were collected on poly-l-lysine coated slides, air-dried overnight at 37 °C and stored at room temperature for subsequent investigation. Sections were dewaxed with xylene, rehydrated in graded ethanol series and DEPC treated water, then washed with water before proteinase K (Sigma–Aldrich) digestion. The concentration of proteinase K (in the range from 0.5 to 2.0 µg/ml) was titrated for thymus tissue and best results were obtained with 1 µg/ml. The digestion was stopped by immersion in cold DEPC water. Acetylation was performed by incubating sections in 0.25% acetic anhydride in 85 mM Tris–HCl buffer containing 0.2% acetic acid and 0.02 M ethylenediaminetetraacetic acid (EDTA) for 10 min. The sections were washed with DEPC water and gradually dehydrated. A dilution profile was performed for the probes with concentrations varying from 0.3 to 0.6 ng/µl and the optimal one resulted 0.45 ng/µl. Following overnight incubation at 45 °C, the sections were washed with 2× saline-sodium citrate (SSC) buffer at room temperature, then with 0.2× SSC at 55 °C for 90 min and incubated in 20 µg/ml RNAaseA in 0.01 M Tris–HCl containing 0.5 M NaCl and 1 mM EDTA for 30 min. Sections were transferred to Buffer 1 (0.1 M Tris containing 0.15 M NaCl and 1% blocking reagent) for 1 h, then to Buffer 2 (0.1 M Tris containing 0.15 M NaCl, 0.5% BSA and 0.3% Triton X-100) for 30 min. The sections were incubated for 2 h at room temperature with alkaline phosphatase-conjugated anti-digoxigenin antibody (Fab fragment; Roche Diagnostic, Germany) diluted 1:1000 in Buffer 2, then washed with 0.1 M Tris containing 0.15 M NaCl and Buffer 3 (0.1 M Tris containing 0.1 M NaCl and 50 mM $MgCl_2$). Bound antibody was localized using nitro blue tetrazolium chloride and 5-bromo-4-chloro-3-indolyl-phosphate (Roche Diagnostic, Germany) incubating the sections overnight at room temperature. Thereafter, sections were washed in distilled water and mounted with 50% glycerol. Light microscopy images were captured using a computer-assisted image analysis system which includes a Zeiss microscope equipped with a colour video camera (Axio Cam MRC, Arese, Milano Italy) and a software package (KS 300 and AxioVision). Measurements of cell diameter were performed in five specimens (and pooled) by an observer unaware of treatments.

2.6 Immunohistochemistry

Whole larvae at 25 dph and post-larvae at 51 and 75 dph, and dissected thymus from 1 year-old juveniles (*N* = 20) were fixed in Bouin's liquid for 7 h at 4 °C, dehydrated in cold graded alcohols and embedded in paraffin wax. Serial sections 7 µm-thick were processed for immunohistochemistry (IHC) by ABC-peroxidase with nickel enhancement as previously described [2]. Sections were incubated for 18 h at room temperature with different primary antibodies: I) mouse monoclonal antibodies against human cytokeratins (CK; clone AE1/AE3, Dako Italia, Milano, Italy) or against rat proliferating cell nuclear antigen (PCNA) p36 protein (PC10; Santa Cruz Biotechnology, CA, USA) diluted 1:1000 in PBS 0.1 M, pH 7.3 containing 5% normal horse serum and 0.1% sodium azide, II) rabbit polyclonal antisera against S-100 protein (Dako) or against vimentin (Abcam, Cambridge, UK) diluted 1:400 and 1:100, respectively, in PBS 0.1 M, pH 7.3 containing 5% normal goat serum and 0.1% sodium azide. The primary antibodies were omitted for negative controls. Thereafter, sections were incubated for 60 min with biotinylated horse anti-mouse or goat anti-rabbit IgG sera (Vector Labs., Burlingame, USA), diluted 1:1000 with PBS containing 0.1% sodium azide and 1% BSA, followed by incubation for 60 min with avidin-biotinylated peroxidase complex (ABC, Vectastain Elite, Vector). Following rinses and staining (diaminobenzidine and nickel enhancement), sections were dehydrated, mounted and examined under bright-field illumination. For each specimen, multiple sets of consecutive sections were differentially immunostained with the antibodies above mentioned. Some sections were stained with May-Grünwald/Giemsa for general histology. Microscopic images were captured and analysed as described above.

2.7 Electrophoresis and Western blotting

The thymus was collected from one year-old juveniles (*N* = 3). A lysate was prepared by homogenization in modified RIPA buffer (50 mM Tris–HCl, pH 7.4 containing 1% Triton X-100, 0.2% sodium deoxycholate, 0.2% sodium dodecylsulfate (SDS), 1 mM sodium EDTA, 1 mM phenylmethylsulfonyl fluoride, 5 µg/ml aprotinin, and 5 µg/ml leupeptin). Tissue and cell debris was pelleted by centrifugation and removed. Protein concentration was determined with Bio-Rad protein assay. The lysate was boiled for 5 min in 1× SDS sample buffer (50 mM Tris–HCl, pH 6.8 containing 12.5% glycerol, 1% SDS, and 0.01% bromophenol blue) added with 5% β-mercaptoethanol. The electrophoresis was performed on 10% polyacrylamide slab minigels by loading whole thymus

lysate (10 µg) in each lane, while proteins ranging from 11 to 170 kDa (Pharmacia Biotech) were used as molecular standards. The gels were stained with Coomassie blue R-250 dye. For Western blots, the gels were blotted onto nitrocellulose for 90 min at 100 mA. The membrane was saturated for 30 min with PBS containing 3% BSA and 0.1% Triton X-100 (PBT), washed with PBS and incubated for 16 h at 25 °C with a rabbit polyclonal antiserum against human S-100 protein (Dako) diluted 1:200 in PBT. The primary antibody was omitted for negative control. After several washes, bound antibody was detected (90 min at room temperature) with horseradish peroxidase-labelled goat anti-rabbit IgG serum (Cappel Europe, Turnhout, Belgium) diluted 1:1000 in PBT, and visualised with 0.02% H_2O_2 and 0.06% 4-chloro-1-naphthol. Coloured molecular standards from 14.3 to 200 kDa (Amersham, Little Chalfont, UK) were used.

2.8 Statistical analysis

Numerical results are expressed as the mean ± SD. One-way ANOVA followed by Bonferroni's multiple comparison test (selected pairs) were used to determine differences among groups. Data analysis was performed using the GraphPad Prism 3.0 software statistical package. The level for accepted statistical significance was $p < 0.05$.

3 Results

3.1 Developmental expression of MHC II-β

Semi-quantitative PCRs were performed on eggs and developing fish from 2 until 92 dph, regarding as well *MHC II-β* transcripts in the thymus of one year-old specimens. RT-PCR analysis for *β-actin* transcripts confirmed the absence of DNA contamination and comparable amounts of mRNA in the different samples (Fig. 1). *MHC II-β* transcripts were first detected at 4 dph, thereafter increased until 92 dph (Fig. 1). Cloning and sequencing of the 4 dph product confirmed sea bass *MHC II-β* identity.

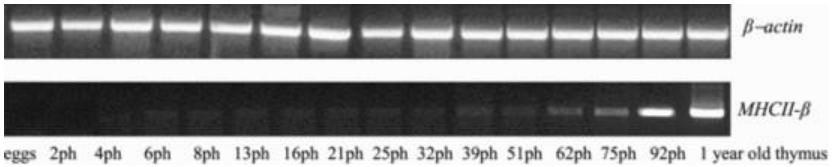

Fig. 1 RT-PCR of *β-actin* and *MHC II-β* transcripts in sea bass eggs, whole larvae and post-larvae. Transcripts in one year-old thymus are shown at the extreme right. *MHC II-β* transcripts were first detected at 4 dph, being undetectable in earlier embryos and released eggs.

The amounts of *MHC II-β* transcripts were quantified by real-time PCR and compared among larvae, post-larvae and thymus of one year-old specimens (Fig. 2). The stage 16 dph, still lacking a morphologically defined thymus, was considered as calibrator. *MHC II-β* transcripts significantly increased ($p < 0.001$) from the 25 dph stage, showing first a lymphoid colonisation of the thymus, thereafter further rose at 51, 75 and 92 dph ($p < 0.001$). At these latter developmental stages the relative amounts of *MHC II-β* transcripts did not show any significant fluctuations. Otherwise, significantly higher levels of *MHC II-β* transcripts were quantified in the 1 year-old thymus compared with all previous stages ($p < 0.001$).

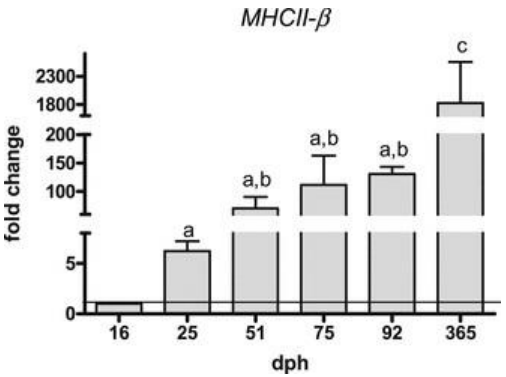

Fig. 2 Real-time PCR of *MHC II-β* transcripts in whole larvae and post-larvae, and one year-old thymus. Data are shown as the mean ± SD of three pools per stage analysed. Significantly different ($p < 0.05$) from [a]16 dph, [b]25 dph, [c]all earlier stages.

3.2 Localization of MHC II-β expressing cells in the developing thymus

Larvae (16 and 25 dph) and post-larvae (51 and 75 dph) were studied by histology, ISH and IHC. No morphologically defined thymic glands were observed in total body sections from 16 dph specimens (Fig. 3a). At 25 dph, paired thymic rudiments with lymphoid appearance were first detected on the dorsal caudal portion of both gill chambers, intimately associated with the pharyngeal epithelium (Fig. 3b). Some MHC II-β^+ cells could be already found, sparse in a subcapsular thymic structure still devoid of any other regional specializations or lobules. Notably, thymic epithelial cells facing the connective tissue (limiting) were devoid of *MHC II-β* transcripts (Fig. 3b). From 25 to 51 dph the organ acquired more complex organization, with progressive establishment of a

cortex from the primordial subcapsular zone, followed by the appearance of a medulla. The penetration of connective trabeculae and accompanying blood vessels into the parenchyma lobulated the thymus and already at 51 dph a distinct cortex/medulla organization was observed in the gland, depicted by differences in cellular density and cytology of lymphoid elements (size, nuclear/cytoplasmic ratio, chromatin pattern) residing in the two regions (Fig. 3c). At this stage numerous MHC II-β^+ cells were mainly restricted to the pharyngeal epithelium and thymic medulla although rare cells were also localized in the cortex (Fig. 3d). Only sparse CK-immunoreactive (IR) cells were found in the thymus and the pharyngeal epithelium (Fig. 3e). These were detected by the mAb AE1/AE3 that recognizes a wide spectrum of CK. At 75 dph a limited increase in number of lymphoid cells was observed (Fig. 4a), mostly localised in the thymic cortex together with sparse, scattered MHC II-β^+ cells. These latter occurred at higher numbers in the medulla (Fig. 4b). At this stage CK-, S100-, and vimentin-IR cells were found in the organ (Fig. 4c–e). In detail, CK-IR cells were detected in the pharyngeal epithelium and sparse in thymic cortex and medulla (Fig. 4c), whereas rare S100- or vimentin-IR cells were found only in the medulla (Fig. 4d–e).

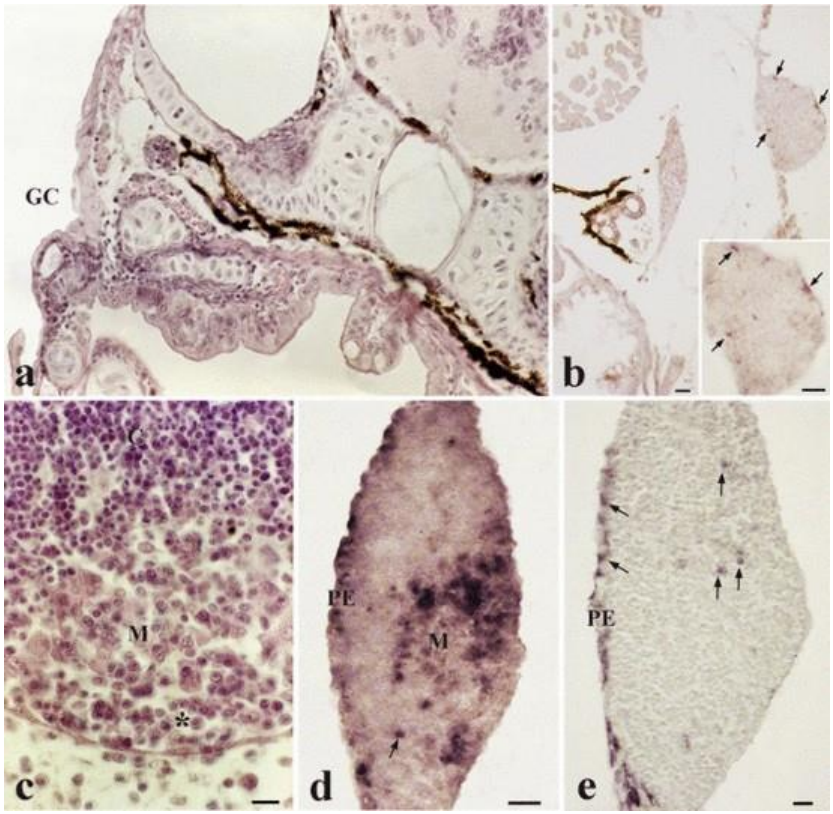

Fig. 3 Histology, ISH and IHC of larvae (16 and 25 dph) and post-larvae (51 dph). Histological analysis of 16 dph specimens did not reveal any thymic glands with lymphoid appearance (~~Fig. 3~~a). At 25 dph, only sparse MHC II-β^+ cells (arrows, showed at higher magnification in the inset) are detected by ISH in the thymic rudiment in continuity with the pharyngeal epithelium (~~Fig. 3~~b). At 51 dph, obvious cortex and medulla regions have developed. The asterisk indicates a subcapsular zone (~~Fig. 3~~c). Numerous cells containing *MHC II-β* transcripts are mainly in the medulla and in the pharyngeal epithelium, although sparse positive cells (arrow) also localize in the cortex (~~Fig. 3~~d). Rare CK-IR cells were found by IHC in the inner thymic zone and pharyngeal epithelium (arrows) (~~Fig. 3~~e). GC: gill chamber; C: cortex; M: medulla; PE: pharyngeal epithelium. Scale bars: 50 µm in (a); 20 µm in (b, d); 30 µm in (c); 10 µm in (e).

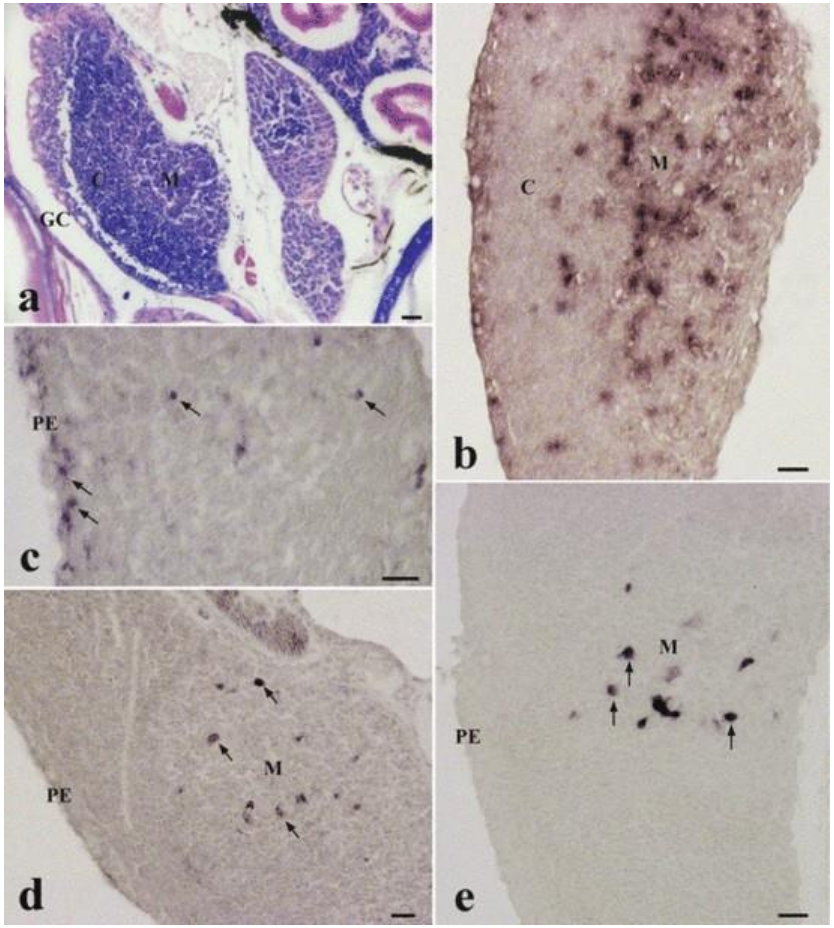

Fig. 4 Histology, ISH and IHC of 75 dph post-larvae. Histological analysis shows a limited increase of lymphoid cells (Fig. 4a) compared with the 51 dph stage (see Fig. 3), mostly localized in the thymic cortex. Sparse MHC II-β^+ cells detected by ISH scatter in the cortex, while are more numerous in the medulla (Fig. 4b). The anti-CK Mab immunostained the pharyngeal epithelium, cTECs and mTECs (arrows) (Fig. 4c). Sparse S100- (Fig. 4d) and vimentin-IR cells (Fig. 4e) detected by IHC were found in the thymic medulla (arrows). GC: gill chamber; C: cortex; M: medulla; PE: pharyngeal epithelium. Scale bars: 20 μm.

The thymus of one year-old specimens was divided into lobules by connective septa coming from the capsule. In each lobule the different density of the thymocytes distinctly drew the cortical and medullary areas while the subcapsular zone was still easily recognizable by the numerous dividing PCNA p36-IR cells (Fig. 5a–c). At this age, MHC II-β^+ cells could be found in each thymic lobule (Fig. 6a), especially numerous in the medulla (Fig. 6b). Although less numerous, these were also detected in the subcapsular and cortical zones of the thymus, as well as in the pharyngeal epithelium, whereas were lacking in the connective septa (Fig. 6a–b). ISH with *MHC II-β* sense probes did not result in any staining, as expected (Fig. 6c).

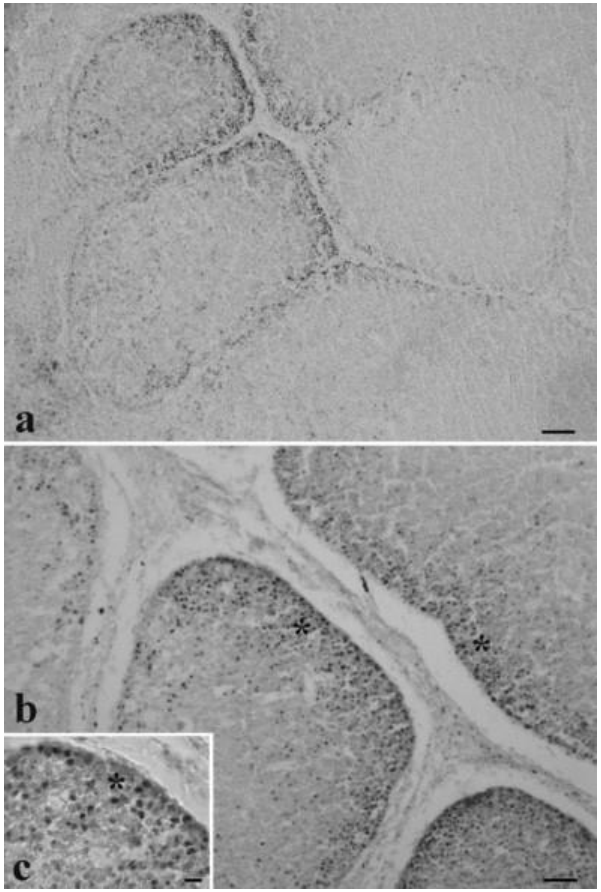

Fig. 5 IHC of thymus from one year-old specimen. The nuclei of numerous proliferating cells are labelled by the anti-PCNA p36 mAb (Fig. 5a). These mainly reside in subcapsular areas (asterisks) (Fig. 5(b) and inset 5(c)). Scale bars: 100 μm in (a); 50 μm in (b); 20 μm in the inset (c).

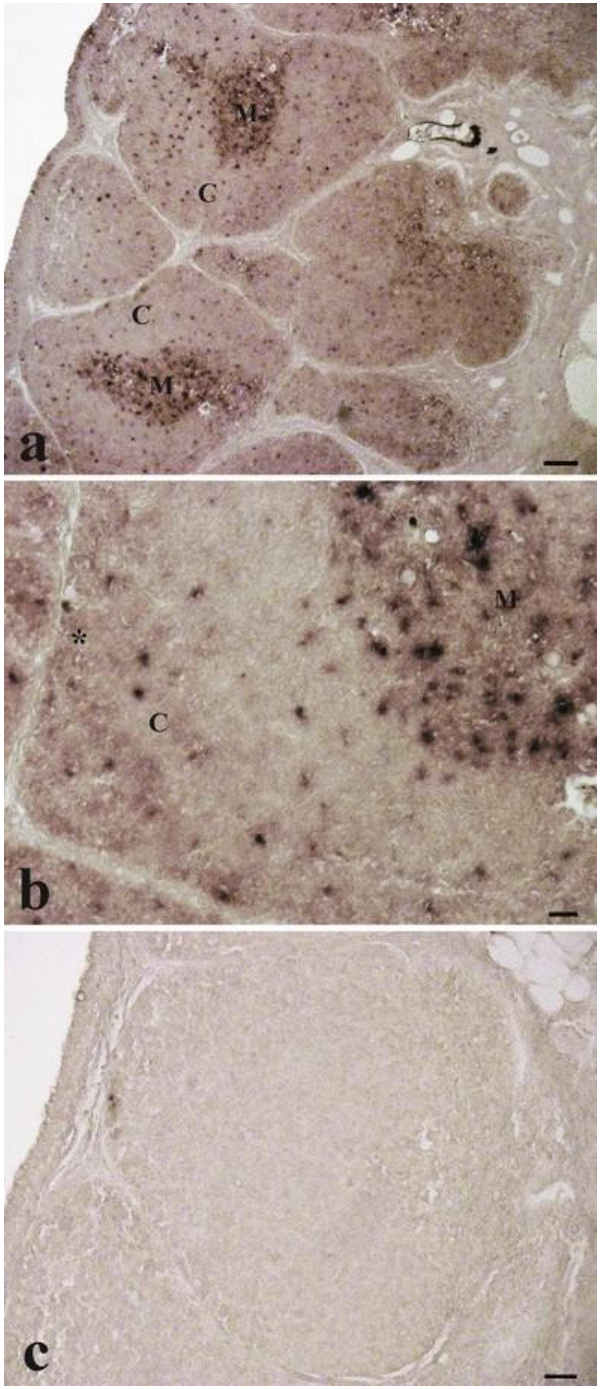

Fig. 6 *MHC II-β* ISH of thymus from one year-old specimen. Positive cells are in the subcapsular zone (asterisk) and in the cortex, but especially numerous in the medulla of each thymic lobule (~~Fig. 6~~(a, ~~Fig. 6~~b) at higher magnification), whereas are lacking in the connective septa. ISH with *MHC II-β*

sense probe is regarded as negative control (Fig. 7c). C: cortex; M: medulla. Scale bars: 100 μm in (a); 20 μm in (b, c).

Adjacent sections were processed either for *MHC II-β* ISH or anti-CK IHC and a staining overlap was recorded for some thymic stromal cells (Fig. 7). The *MHC II-β* anti-sense probe stained cells with patent cytoplasmic extensions scattered in the cortex (Fig. 6a), that is with typical morphology and localization of cTECs, also evidenced by their CK immunolabeling (Fig. 7b), although they accounted for only a fraction of total sea bass cTECs. A staining overlap for MHC II-β and CK was also found in stromal cells, apparently isolated but disposed in an ordered fashion parallel to the capsule, along the subcapsular zone of the thymus (Fig. 7c–d). Otherwise, the TECs facing the connective tissue (subcapsular and peritrabecular) were obviously CK-IR but lacked any detectable *MHC II-β* transcripts (Fig. 7e–f). In the medulla, numerous MHC II-β^+ cells were found (Fig. 7g) as well as CK-IR mTECs (Fig. 7h). It is worth noting that also CK-IR perivascular TECs in the medulla contained abundant *MHC II-β* transcripts (Fig. 7i–j).

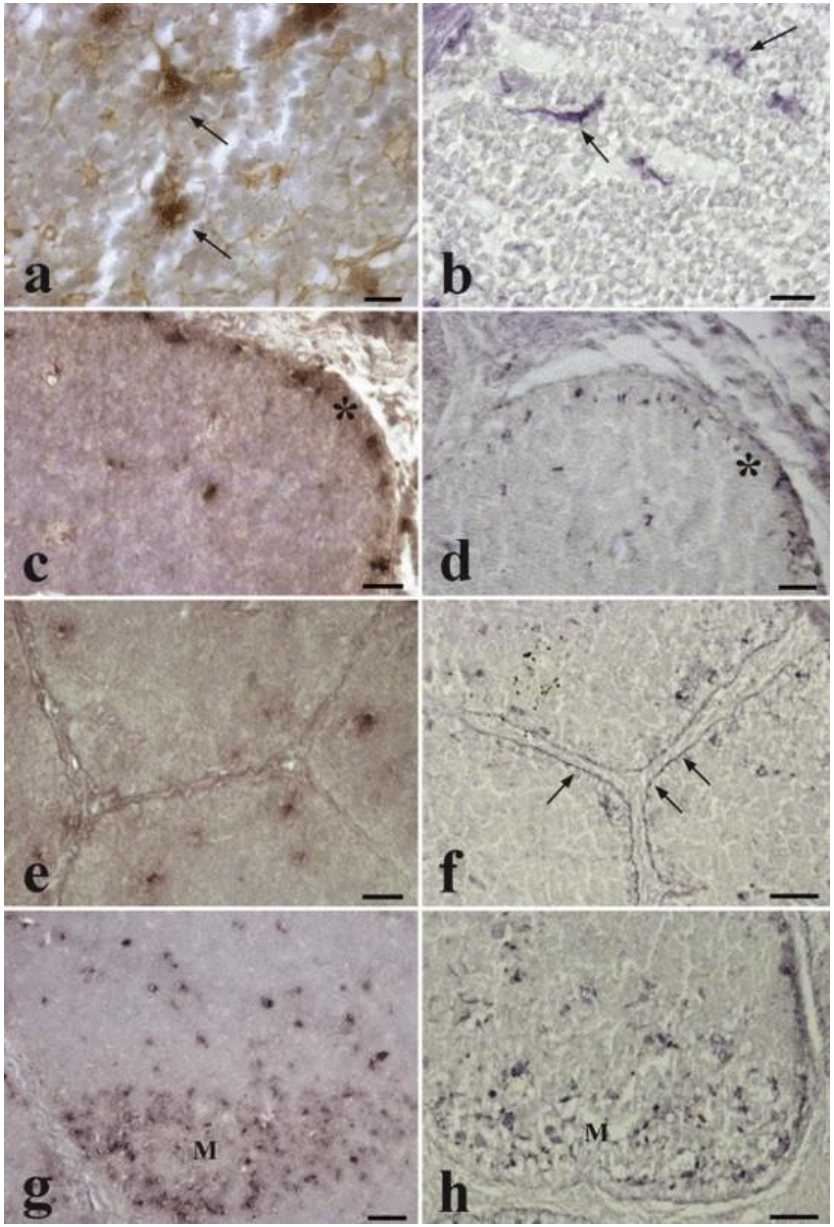

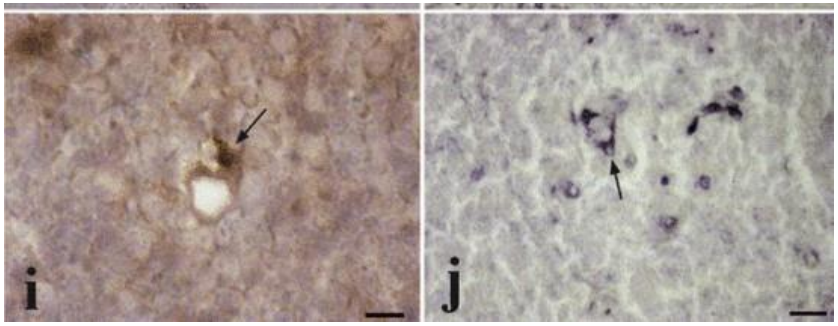

Fig. 7 *MHC II-β* ISH and anti-CK immunostaining of adjacent sections of one year-old thymus. *MHC II-β* anti-sense probe stains scattered cortical cells with typical morphology and localization of reticular TECs (~~Fig. 7~~a), as denoted by their CK immunolabeling (~~Fig. 7~~b). MHC II-β^+ cells are also detected in the subcapsular zone (asterisk) (~~Fig. 7~~c), again apparently CK-IR (~~Fig. 7~~d). Otherwise, no detectable *MHC II-β* transcripts are found in CK-IR subcapsular TECs facing the connective tissue (~~Fig. 7~~e, f). MHC II-β^+ positive cells are rather numerous in the medulla (~~Fig 7~~g), largely housed by CK-IR stromal cells (~~Fig. 7~~h). MHC II-β^+ perivascular cells (~~Fig. 7~~i), also CK-IR (~~Fig. 7~~j), are also detected in the medulla. Scale bars: 20 μm in (a, d, e, j); 10 μm in (b); 50 μm in (f); 40 μm in (g, h); 5 μm in (i).

Adjacent sections were processed either for *MHC II-β* ISH (Fig. 8a) or IHC with antisera against S-100 protein (Fig. 8b) or vimentin (Fig. 8c). MHC II-β^+ cells scattered in the subcapsular and cortical thymic zones lacked both S-100 and vimentin immunostaining. Otherwise, medullary cells MHCII-β^+ and S100-IR resulted remarkably similar according to localization, cellular features and diameter (6.62 ± 0.59 μm and 8.05 ± 3.87 μm, respectively, N = 100 per group). They were especially concentrated at the cortico-medullary border (CMB). (Fig. 8d–f). Vimentin-IR medullary cells were apparently less numerous and had larger size (12.77 ± 7.46 μm) compared with MHC II-β^+ and S100-IR cells ($p < 0.01$). It is worth noting that also macrophages within intra-thymic melano-macrophage centres were vimentin-IR, while were lacking any detectable *MHC II-β* transcripts or S-100 immunolabeling (Fig. 8g–i).

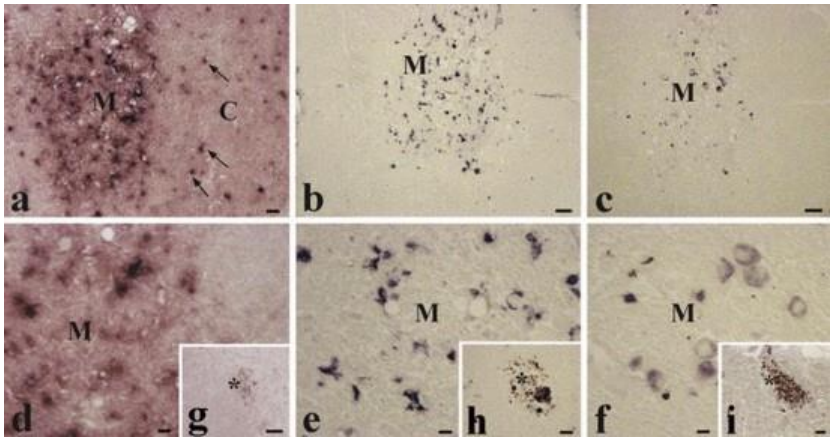

Fig. 8 *MHC II-β* ISH, and S-100 or vimentin immunostaining of adjacent sections of one year-old thymus. Note the concentration of MHC II-β^+ (~~Fig. 8~~a), S100-IR (~~Fig. 8~~b) and vimentin-IR cells (~~Fig. 8~~c) in the medulla, where the two former largely overlap in number and cell size, whereas the latter appear evidently less numerous and of larger size. Note also the occurrence in the thymic cortex of only MHC II-β^+ stromal cells (arrows) (~~Fig. 8~~a). Higher magnifications showing MHC II-β^+ (~~Fig. 8~~d), S100-IR (~~Fig. 8~~e) and vimentin-IR cells (~~Fig. 8~~f) in the medulla. The macrophages within the melano-macrophage centres (asterisk) occurring in the thymus lacked any detectable *MHC II-β* transcripts (inset ~~8~~(g)) and S-100 immunolabeling (inset ~~8~~(h)), whereas were vimentin-IR (inset ~~8~~(i)). The melanin pigment is not a result of immunostaining. C: cortex; M: medulla. Scale bars: 20 μm in (a); 50 μm in (b, c); 10 μm in (d–f); 50 μm in (g); 20 μm in (h–i).

3.3 Electrophoresis and Western blotting of the thymus lysate

The thymus lysate from one year-old juveniles was used for electrophoresis and Western blot analysis (Fig. 9). The rabbit polyclonal antiserum against S-100 immunolabeled a 20–30 kDa band (see lane 2), that is of predicted size. No bands were ~~labeled~~ labelled in negative control (not shown).

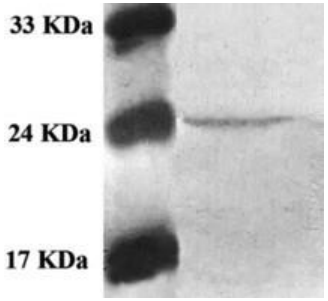

Fig. 9 Western blot analysis of whole thymus lysate from one year-old juvenile. Coloured molecular standards from 14.3 to 200 kDa are shown in the left lane. The polyclonal antiserum against S-100 immunolabeled a 20–30 kDa band (right lane).

4 Discussion

MHC molecules are crucial for T cell development, as demonstrated by low production of $CD8^+$ or $CD4^+$ cells in class $I^{-/-}$ or class $II^{-/-}$ mice [13,23,30,64]. Whereas class I molecules are expressed by all nucleated cells, the class II ones are exposed only by a limited subgroup, including TECs and other 'professional' APCs. This study aimed at interpretating measurable variations of *MHC II-β* transcripts and their dynamics throughout sea bass development, as well as the distribution of positive cells in the different zones of the thymus, comparing it to the histological organization of mammalian thymus.

An early appearance of *MHC II-β* transcripts was found in 4 dph larvae, notably 3 weeks before the first lymphoid appearance of the thymus ([41,42] and this paper). These findings recall earlier data gathered in common carp, in which *MHC II-β* transcripts were detected at the day 1 post-fertilization [45], three days before thymus appearance [48]. Cells of the hematopoietic lineage, i.e. macrophages, that appear earlier than thymus in many vertebrates could account for this early expression. Phagocytic activity was in fact detected in the zebrafish embryo prior to hatching [27] and at the day 2 post-fertilization in the carp embryo [46]. Similarly, an early appearance of macrophages has been described in other teleost species [11,24]. Also in the mouse, the MHC II molecules appear very early in organogenesis and can even be reliable markers to monitor differentiation of the thymic epithelium. In fact, its first developmental phase can occur in the absence of lymphoid progenitors that, when immigrated into the stromal anlage, later induce surface expression of MHC class I and class II molecules by TECs [28].

From 4 dph onward the amounts of *MHC II-β* transcripts increased until the 25 dph stage, when the first lymphoid colonization of the thymus was recorded, and became significantly different compared with all previous stages analysed. It appears likely that the 25 dph thymus might contribute to the overall increase of the *MHC II-β* transcripts, and provide the proper microenvironment to support early phases of thymocyte development, as shown by the occurrence of first detectable *TCR-β* transcripts [42]. *MHC II-β* ISH detected sparse cells in the thymic anlage, still devoid of any lobules or regional specializations, similarly to what reported in mouse in which the epithelial cell compartments are not clearly defined in the initial thymic rudiment [28]. In fact, although T-cell progenitors enter the mouse thymus by day 11th, the organ does not differentiate into cortex and medulla regions before day 13th of gestation [5659]. In particular the medullary structure, whose formation is influenced by more differentiated thymocytes [58], is formed last.

From 25 to 51 dph the sea bass thymus progressively developed from the primordial subcapsular zone (that would be later defined as an outer cortex) a cortex filled by small thymocytes, followed by the appearance of a medulla [42]. Previous studies have demonstrated that 51 dph is indeed a crucial stage for development of this regionalization and transitional stages of thymocyte maturation. At this stage first expression of the T cell coreceptors CD4 and CD8α was recorded [41,42] and *MHC II-β* transcripts significantly increased compared with earlier stages, not rising further up to 92 dph. Regarding the thymic architecture, we detected at 51 dph a medullary organization [1,41,42], associated to the patent penetration into the parenchyma of connective septa coming from the inner capsule. At this stage *MHC II-β* transcripts were localized in cells scattered in the thymic subcapsular zone and cortex (and pharyngeal epithelium), but in particular in medullary stromal cells. For at least some of these latter an epithelial nature was indicated by CK immunolabeling, but most could represent precursor mesenchymal cells still lacking S-100 or vimentin expression [6,20,21,36,50]. The sea bass thymus is in continuity with the pharyngeal epithelium throughout development and the occurrence of MHC II-β^+ cells at this latter location deserves attention. A very recent study showed that also in rainbow trout cells expressing MHC II localize both inside the thymus and in the epithelium of the gill chamber (as well as in epidermis, intestine, gills and pseudobranch) [26]. These were interpreted by the Authors as tissue resident macrophages, however a precise characterization of these cells is still lacking in both species and the hypothesis about a (unknown) functional role in thymocyte selection should not be discarded.

It is known that mammalian TECs are phenotypically and functionally heterogenous, and reside in distinct areas of cortex and medulla. Indeed, cTECs and mTECs exert cooperative roles to provide essential signals for specific stages of T cell development [29]. The successful generation of a mature and self-tolerant T cell repertoire requires that developing thymocyes pass at least two checkpoints: positive and negative selection. Results gathered in developing sea bass indicate that the 51 dph thymocyes, mostly residing in the cortex and already transcribing CD4 and CD8α [41,42], possibly archived the process known as positive selection. This could be mediated by cTECs, allowing T lineage cells, that have rearranged a TCR capable of recognizing self peptide-MHC II complexes at appropriate affinity, to survive and commit to the $CD4^+$ lineage (as for others to the $CD8^+$ one after appropriate MHC I engagement), in the sea bass as it has been reported in mammals. It would be assumed that a nearly complete operative system regulating sea bass thymocyte differentiation steps constitute together with medullary differentiation.

The sea bass thymic stromal cells apparently differentiate according to a definite developmental timing, as detailed in the murine thymus, in which TECs expressing MHC class II appear earlier than stromal cells of mesenchymal origin [32]. This progressive organization of the thymic architecture suggests the onset of adaptations to different functions during ontogeny. At 75 dph we first immunodetected in sparse medullary cells vimentin, the major intermediate filament protein in a variety of mesenchymal cells including macrophages, and the calcium binding protein S-100, a well known molecular marker for DCs [15,20,21,43,50]. Especially for these putative DCs a key role in negative selection to remove highly self-reactive thymocytes appears likely, even if an additional role in this process of other populations of medullary stromal cells, as described in mouse ([25], Jenkinson et al., 1994), should not be excluded. Apoptotic thymocytes, first detected at 35 dph in the sea bass thymus, significantly increased in number, notably concentrated at the CMB, only at 74 dph [1] that is almost the time showing appearance of specialised non-epithelial medullary stromal cells. Macrophages engulfing apoptotic cells or bodies are observed very frequent, especially at the CMB [1], in the sea bass thymus, that contains high transcripts amounts of *MIF*, a factor crucially relevant to retain *in loco* the thymic macrophages [8]. A major role in the clearing of apoptotic cells [18,54] can be hypothesized for these cells, most likely unable to perform negative selection of potentially autoreactive thymocytes [60].

High amounts of *MHC II* transcripts were detected in the thymus of 1 year-old fish, indicating that thymocyte differentiation and selection processes would be fully operative. Indeed, these sea bass individuals were still immature, and a thymus involution associated with sexual maturity or aging has not been clearly documented so far. Even indications about a lifelong persistence of the primary lymphoid function of the teleost thymus have derived from permanent *RAG1* and *RAG2* transcription in common carp [7]. In one year-old sea bass the thymus was subdivided by connective septa into lobules, each one distinctly compartmentalized into cortex and medulla zones housing highly different numbers of thymocytes. The subcapsular zone was easily recognizable by the occurrence of numerous dividing cells identified by immunolabeling of PCNA p36, a protein highly conserved throughout evolution (from yeasts to mammals) and synthesized by proliferating cells (in early G_1 and S phases of the cell cycle). MHC II-β^+ cells resided in each thymic lobule: scattered in the subcapsular and cortical zones (as well as in the pharyngeal epithelium, whereas lacking in the connective septa), but especially numerous in the medulla. Also in the thymus of Atlantic salmon MHC IIβ-IR cells were mainly in the medulla, and to a lower degree in the cortex [31], in agreement with the distribution previously described in amphibians [17] and mammals. At difference with the thymus of some mammalian species, MHC II-β expression in teleosts appeared limited to a lower number of cortical stromal cells. It is worth mentioning that MHC II amount in mouse cTECs, possibly due to masking by thymocytes, is greater than previously thought [62], although cTECs are less numerous than mTECs and DCs in the medulla, where thymocytes number is lower. In particular, MHC II molecules were shown to form distinct focal aggregates on the surface of cTECs (not on mTECs), suggesting that these could constitute a functional unit at much higher local concentration to yield a higher avidity interaction with TCR [62].

It appears likely from our results that also in the sea bass MHC II-β^+ cTECs would be involved in the positive selection of thymocytes. In the cortex, apparently overlapped detection of *MHC II* transcripts and CK immunolabeling provided evidence for the epithelial nature of such stromal cells, and the same applied for those MHC II-β^+ in the subcapsular zone and some medullary cells, including perivascular TECs. These observations denote that the sea bass TECs would subserve functionally distinct thymic areas as described in mammals [29]. *MHC II-β* ISH was distinctly stronger in the medulla, and we attribute very high relevance to the detection of a major population of MHC II-β^+ stromal cells, a fraction of which, of similar cell size, was also immunolabeled with the antiserum against S-100, a molecular marker of DCs. In trout, DCs apparently possess many of the hallmarks of the mammalian counterparts: arborized morphology, expression of specific molecular markers, ability to phagocytose small particles, activation by TLR ligands, ability to migrate *in vivo*, and abundant *CD83* and *MHC II* transcripts [6]. Also in zebrafish some cells were identified as expressing genes, including *IL-12*, *MHC II iclp1*, and *csf1r* [36], associated with DCs function and antigen presentation. The findings gathered in these two species suggested that mechanisms involved in specialised antigen presentation could be remarkably conserved throughout the evolution of jawed vertebrates. We report about the specific localization in the sea bass thymic medulla, and notably at the CMB, of DCs that could exert a key control of thymocyte negative selection. These observations would produce significant advancements in the field of teleost immunobiology, while future studies will be devoted at detailing the ultrastructural features of these cells, exploring by appropriate tools their origin and developmental pathways and defining their functional role.

In general terms, our study reports about the specialization of the sea bass thymic microenvironments during development, to support various differentiation steps that ultimately lead to maturation of naïve T cells. The reports that in one year-old sea bass near all cortical thymocytes express both CD4 and CD8 (double positive), while the medullary ones either coreceptor (single positive) have provided almost definitive proof [41]. The patterns of *MHC II* expression by TECs and DCs suggest that efficient mechanisms of positive and negative selection of T cells would be operative, strongly reminiscent of well characterised models conserved in more evolved gnathostomes.

Uncited reference

[4,59].

Acknowledgements

The authors wish to thank the staff of the Aquaculture station "Civitaittica", Civitavecchia (Italy), for help in fish handling. This research was partially funded by the European Commission under the 7th Framework Programme for Research and Technological Development (FP7) of the European Union (Grant Agreement 311993 TARGETFISH) and by the PRIN Project 20109XZEPR-010.

References

[1]

L. Abelli, M.R. Baldassini, R. Meschini and L. Mastrolia, Apoptosis of thymocytes in developing sea bass *Dicentrarchus labrax* (L.), *Fish Shellfish Immunol* 8, 1998, 13–24.

[2]

L. Abelli, V.P. Gallo, A. Civinini and L. Mastrolia, Immunohistochemical and ultrastructural evidence of adrenal chromaffin cell subtypes in sea bass *Dicentrarchus labrax* (L.), *Gen Comp Endocrinol* 102, 1996, 113–122.

[3]

O. Archer and J.C. Pierce, Role of thymus in development of the immune response, *Fed Proc* 1961, 20–26.

[4]

B.G. Arnason, B.D. Jakovic and B.H. Waksman, Effect of thymectomy on 'delayed' hypersensitive reactions, *Nature* 194, 1962, 99–100.

[5]

B. Bajoghli, N. Aghaallaei, I. Hess, I. Rode, N. Netuschil, B.H. Tay, et al., Evolution of genetic networks underlying the emergence of thymopoiesis in vertebrates, *Cell* 138, 2009, 186–197.

[6]

E. Bassity and T.G. Clark, Functional identification of dendritic cells in the teleost model, rainbow trout (*Oncorhynchus mykiss*), *PLoS One* 7, 2012, e33196.

[7]

T.J. Bowden, P. Cook and J.H.W.M. Rombout, Development and function of the thymus in teleosts, *Fish Shellfish Immunol* 19, 2005, 413–427.

[8]

F. Buonocore, E. Randelli, A.M. Facchiano, A. Pallavicini, M. Modonut and G. Scapigliati, Molecular and structural characterization of a macrophage migration inhibitory factor from sea bass (*Dicentrarchus labrax* L.), *Vet Immunol Immunopathol* 136, 2010, 297–304.

[9]

F. Buonocore, E. Randelli, D. Casani, S. Costantini, A. Facchiano, G. Scapigliati, et al., Molecular cloning, differential expression and 3D structural analysis of the MHC class-II β chain from sea bass (*Dicentrarchus labrax* L.), *Fish Shellfish Immunol* 23, 2007, 853–866.

[10]

F. Buonocore, L. Randelli, S. Bird, C. Secombes, S. Constantini, A. Facchiano, et al., The CD8α from sea bass (*Dicentrarchus labrax* L.): cloning, expression and 3D modelling, *Fish Shellfish Immunol* 20, 2006, 637–646.

[11]

C. Chantanachookhin, T. Seikai and M. Tanaka, Comparative study of the ontogeny of the lymphoid organs in three species of marine fish, *Aquaculture* 99, 1991, 143–155.

[12]

S.L. Chen, Y.X. Zhang, M.Y. Xu, X.S. Ji, G.C. Yu and C.F. Dong, Molecular polymorphism and expression analysis of MHC class II B gene from red sea bream (*Chrysophrys major*), *Dev Comp Immunol* 30, 2006, 407–418.

[13]

D. Cosgrove, D. Gray, A. Dierich, J. Kaufman, M. Lemeur, C. Benoist, et al., Mice lacking MHC class II molecules, *Cell* 66, 1991, 1051–1066.

[14]

A. Cuesta, A.M. Esteban and J. Meseguer, Cloning, distribution and up-regulation of the teleost fish MHC class II alpha suggests a role for granulocytes as antigen-presenting cells, *Mol Immunol* 43, 2006, 1275–1285.

[15]

A.J. Demetris, C. Sever, S. Kakizoe, S. Oguma, T.E. Starzl and R. Jaffe, S100 protein positive dendritic cells in primary biliary cirrhosis and other chronic inflammatory liver diseases, *Am J Pathol* 134, 1989, 741–747.

[16]

B. Dixon, L.A.J. Nagelkerke, F.A. Sibbing, E. Egberts and R.J.M. Stet, Evolution of MHC class II b chain-encoding genes in the Lake Tana barbell species flock (*Barbus intermedius* complex), *Immunogenetics* 44, 1996, 419–431.

[17]

L. Du Pasquier and M.F. Flajnik, Expression of MHC class II antigens during *Xenopus* development, *Dev Immunol* 1, 1990, 85–95.

[18]

V.A. Fadok, D.R. Voelker, P.A. Campbell, J.J. Cohen, D.L. Bratton and P.M. Henson, Exposure of phosphatidylserine on the surface of apoptotic lymphocytes triggers specific recognition and removal by macrophages, *J Immunol* 148, 1992, 2207–2216.

[19]

F. Figueroa, W.E. Mayer, H. Sultmann, C. O'Huigin, H. Tichy, Y. Satta, et al., MHC class II B gene evolution in East African cichlid fishes, *Immunogenetics* 51, 2000, 556–575.

[20]

M. Gallego, E. del Cacho, C. Arnal, C. Felices, E. Lloret and J.A. Bascuas, Immunocytochemical detection of dendritic cell by S-100 protein in the chicken, *Eur J Histochem* 36, 1992, 205–213.

[21]

M. Gallego, I. Olah, E. del Cacho and B. Glick, Anti S-100 antibody recognizes ellipsoid-associated cells and other dendritic cells in the chicken spleen, *Dev Comp Immunol* 17, 1993, 77–83.

[22]

R. Graser, C. O'Huigin, V. Vincek, A. Meyer and J. Klein, Trans-species polymorphism of class II MHC loci in danio fishes, *Immunogenetics* 44, 1996, 36–48.

[23]

J.M. Grusby, S.R. Johnson, E.V. Papaioannou and L.H. Glimcher, Depletion of $CD4^+$ T cells in major histocompatibility complex class II-deficient mice, *Science* 253, 1991, 1417–1420.

[24]

P.C. Hanington, J. Tam, B.A. Katzenback, S.J. Hitchen, D.R. Barreda and M. Belosevic, Development of macrophages of cyprinid fish, *Dev Comp Immunol* 33, 2009, 411–429.

[25]

K.J. Hare, J. Pongracz, E.J. Jenkinson and G. Anderson, Modeling TCR signaling complex formation in positive selection, *J Immunol* 171, 2003, 2825–2831.

[26]

R.D. Heinecke, J.K. Chettri and K. Buchmann, Adaptive and innate immune molecules in developing rainbow trout, *Oncorhynchus mykiss* eggs and larvae: expression of genes and occurrence of effector molecules, *Fish Shellfish Immunol* 38, 2014, 25–33.

[27]

P. Herbomel, B. Thisse and C. Thisse, Ontogeny and behaviour of early macrophages in the zebrafish embryo, *Development* 126, 1999, 3735–3745.

[28]

E.J. Jenkinson, W. Van Ewijk and J.J. Owen, Major histocompatibility complex antigen expression on the epithelium of the developing thymus in normal and nude mice, *J Exp Med* 153, 1981, 280–292.

[29]

S.R. Jenkinson, S. Zuklys, G.A. Hollander, P.A. Koni, B. Reizis and R.J. Hodes, Importance of MHCII expression on thymic epithelium versus dendritic cells for the positive and negative selection of CD4 T cells, *J Immunol* 182, 2009, (Meeting Abstract Supplement) 138.28.

[30]

B.H. Koller, P. Marrack, J.W. Kappler and O. Smithies, Normal development of mice deficient in β2M, MHC class I proteins, and $CD8^+$ T cells, *Science* 248, 1990, 1227–1230.

[31]

E.O. Koppang, I. Hordvik, I. Bjerkås, J. Torvund, L. Aune, J. Thevarajan, et al., Production of rabbit antisera against recombinant MHC class II β chain and identification of immunoreactive cells in Atlantic salmon (Salmo salar), *Fish Shellfish Immunol* 14, 2003, 115–132.

[32]

G. Kraal, L. Avis, J. Wijffels, K. Hoeben and H. ter Hart, Different epitopes on the dendritic cell-associated NLDC-45 molecule during ontogeny, *Immunobiology* 181, 1990, 388–397.

[33]

E. Ladi, X. Yin, T. Chtanova and E.A. Robey, Thymic microenvironments for T cell differentiation and selection, *Nat Immunol* 7, 2006, 338–343.

[34]

D.M. Langenau and L.I. Zon, The zebrafish: a new model of T-cell and thymic development, *Nat Rev Immunol* 5, 2005, 307–317.

[35]

H. Li, L. Jiang, J. Han, H. Su, Q. Yang and C. He, Major histocompatibility complex class IIA and IIB genes of the spotted halibut *Verasper variegatus*: genomic structure, molecular polymorphism, and expression analysis, *Fish Physiol Biochem* 37, 2011, 767–780.

[36]

G. Lugo-Villarino, K.M. Balla, D.L. Stachura, K. Bañuelos, M.B.F. Werneck and D. Traver, Identification of dendritic antigen-presenting cells in the zebrafish, *Proc Natl Acad Sci U S A* 107, 2010, 15850–15855.

[37]

M.M. Martinic, M.F. Van Den Broek, T. Rülicke, C. Huber, B. Odermatt, W. Reith, et al., Functional $CD8^+$ but not $CD4^+$ T cell responses develop independent of thymic epithelial MHC, *Proc Natl Acad Sci U S A* 103, 2006, 14435–14440.

[38]

J.F. Miller, Immunological function of the thymus, *Lancet* 2, 1961, 748–749.

[39]

K.M. Miller and R.E. Withler, Sequence analysis of a polymorphic MHC class II gene in Pacific salmon, *Immunogenetics* 43, 1996, 337–351.

[40]

A.C. Øvergård, I.U. Fiksdal, A.H. Nerland and S. Patel, Expression of T-cell markers during Atlantic halibut (*Hippoglossus hippoglossus* L.) ontogenesis, *Dev Comp Immunol* 35, 2011, 203–213.

[41]

S. Picchietti, L. Guerra, F. Buonocore, E. Randelli, A.M. Fausto and L. Abelli, Lymphocyte differentiation in sea bass thymus: CD4 and CD8-α gene expression studies, *Fish Shellfish Immunol* 27, 2009, 50–56.

[42]

S. Picchietti, L. Guerra, L. Selleri, F. Buonocore, L. Abelli, L. Scapigliati, et al., Compartmentalisation of T cells expressing CD8α and TCRβ in developing thymus of sea bass *Dicentrarchus labrax* (L.), *Dev Comp Immunol* 32, 2008, 92–99.

[43]

P.L. Poliani, F. Facchetti, M. Ravanini, A.R. Gennery, A. Villa, C.M. Roifman, et al., Early defects in human T-cell development severely affect distribution and maturation of thymic stromal cells: possible implications for the pathophysiology of Omenn syndrome, *Blood* 114, 2009, 105–108.

[44]

S.S. Ristow, L.D. Grabowski, S.M. Thompson, G.W. Warr, S.L. Kaattari, J.M. de Avila, et al., Coding sequences of the MHC II b chain of homozygous rainbow trout (*Oncorhynchus mykiss*), *Dev Comp Immunol* 23, 1999, 51–60.

[45]

P.N.S. Rodrigues, T.T. Hermsen, A. van Maanen, A.J. Taverne-Thiele, J.H.W.M. Rombout, B. Dixon, et al., Expression of MhcCyca class I and class II molecules in the early life history of the common carp (*Cyprinus carpio* L.), *Dev Comp*

Immunol 22, 1998, 493–506.

[46]

N. Romano, S. Picchietti, J.J. Taverne-Thiele, N. Taverne, L. Abelli, L. Mastrolia, et al., Distribution of macrophages during fish development: an immunohistochemical study in carp (*Cyprinus carpio*, L.), *Anat Embryol* 198, 1998, 31–41.

[47]

A. Sato, R. Dongak, L. Hao, S. Shintani and T. Sato, Organization of Mhc class II A and B genes in the tilapiine fish *Oreochromis*, *Immunogenetics* 64, 2012, 679–690.

[48]

C.J. Secombes, J.J. van Groningen, W.B. van Muiswinkel and E. Egberts, Ontogeny of the immune system in carp (*Cyprinus carpio* L.). The appearance of antigenic determinants on lymphoid cells detected by mouse anti-carp thymocyte monoclonal antibodies, *Dev Comp Immunol* 7, 1983, 455–464.

[49]

T. Shen, S. Xu and M. Yang, Molecular cloning, expression pattern, and 3D structural analysis of the MHC class IIB gene in the Chinese longsnout catfish (*Leiocassis longirostris*), *Vet Immunol Immunopathol* 141, 2011, 33–45.

[50]

R.M. Steinman, M. Pack and K. Inaba, Dendritic cells in the T-cell areas of lymphoid organs, *Immunol Rev* 156, 1997, 25–37.

[51]

R.J.M. Stet, B. de Vries, K. Mudde, T. Hermsen, J. van Heerwaarden, B.P. Shump, et al., Unique haplotypes of co-segregating major histocompatibility class II A and class II B alleles in Atlantic salmon (*Salmo salar*) give rise to diverse class II genotypes, *Immunogenetics* 54, 2002, 320–331.

[52]

R.J.M. Stet, C.P. Kruiswijk, J.P.J. Saeij and G.F. Wiegertjes, Major histocompatibility genes in cyprinid fishes: theory and practice, *Immunol Rev* 166, 1998, 301–316.

[53]

H. Sultmann, W.E. Mayer, F. Figueroa, C. O'Huigin and J. Klein, Zebrafish MHC class II α chain-encoding genes: polymorphism, expression, and function, *Immunogenetics* 38, 1993, 408–420.

[54]

C.D. Surh and J. Sprent, T-cell apoptosis detected in situ during positive and negative selection in the thymus, *Nature* 372, 1994, 100–103.

[55]

F. Takizawa, J.M. Dijkstra, P. Kotterba, T. Korytář, H. Kock, B. Köllner, et al., The expression of CD8α discriminates distinct T cell subsets in teleost fish, *Dev Comp Immunol* 35, 2011, 752–763.

[56]

H. Toda, K. Araki, T. Moritomo and T. Nakanishi, Perforin-dependent cytotoxic mechanism in killing by CD8 positive T cells in ginbuna crucian carp *Carassius auratus langsdorfii*, *Dev Comp Immunol* 35, 2011a, 88–93.

[57]

H. Toda, Y. Saito, T. Koike, F. Takizawa, K. Araki, T. Yabu, et al., Conservation of characteristics and functions of CD4 positive lymphocytes in a teleost fish, *Dev Comp Immunol* 35, 2011b, 650–660.

[58]

W. van Ewijk, E.W. Shores and A. Singer, Crosstalk in the mouse thymus, *Immunol Today* 15, 1994, 214–217.

[59]

E. van Vliet, E.J. Jenkinson, R. Kingston, J.J.T. Owen and W. Van Ewijk, Stromal cell types in the developing thymus of the normal and nude mouse embryo, *Eur J Immunol* 15, 1985, 675–681.

[60]

A. Volkmann, T. Zal and B. Stockinger, Antigen-presenting cells in the thymus that can negatively select MHC class II-restricted T cells recognizing a circulating self antigen, *J Immunol* 158, 1997, 693–706.

[61]

R.B. Walker, T.J. McConnell and R.A. Walker, Variability in a MHC Mosa class II beta chain-encoding gene in striped bass (*Morone saxatilis*), *Dev Comp Immunol* 18, 1994, 325–342.

[62]

S.Y. Yang, S. Ahn, C.S. Park, K.L. Holmes, J. Westrup, C.H. Chang, et al., The quantitative assessment of MHC II on thymic epithelium: implications in cortical thymocyte development, *Int Immunol* 18, 2006, 729–739.

[63]

A. Zapata and C.T. Amemiya, Phylogeny of lower vertebrates and their immunological structures, *Curr Top Microbiol* 248, 2000, 67–107.

[64]

M. Zijlstra, M. Bix, N.E. Simister, J.M. Loring, D.H. Raulet and R. Jaenisch, β2-microglobulin deficient mice lack $CD4^{-}8^{+}$ cytolytic T cells, *Nature* 344, 1990, 742–746.

Highlights

- *MHC II-β* real-time PCR and ISH detailed thymic development and regionalization.
- Thymocyte selection depends on evolving patterns of *MHC II-β* expression.
- *MHC II-β*$^{+}$ cTECs and medullary dendritic cells are likely involved in thymocyte selection.

Queries and Answers

Query: The following reference is not listed: [Arnason et al. 1961, Stet et al. 2003, Jenkinson et al. 1994]. Please check.

Answer: The right numbering of the first two refs was inserted in the text, the third one was deleted.

Query: Please check the page range in Ref. [36] and correct if necessary.

Answer: the pages are correct.

Query: Please check the layout of Table 1 and correct if necessary.

Answer: ok

Query: Uncited references: This section comprises references that occur in the reference list but not in the body of the text. Please cite each reference in the text or, alternatively, delete it. Any reference not dealt with will be retained in this section.

Answer: Both references are now correctly quoted and numbered in the text.

Query: Please confirm that given names and surnames have been identified correctly.

Answer: Yes